Chapter 14
Recycled Ti-17 Based Composite Design; Optimization Process Parameters in Wire Cut Electrical Discharge Machining (WEDM)

Sonia Ezeddini, Mohamed Boujelbene, Emin Bayraktar, and Sahbi Ben Salem

Abstract This work present a comprehensive study on the effect and optimization of machining parameters on the kerf (cutting width) and material removal rate (MRR) in wire electrical discharge machining (WEDM) process by using the response surface methodology (RSM) and Taguchi method. The experimental studies were conducted under varying parameters. The main input parameters on this model are the cutting parameters such us pulse on time (T_{on}), servo voltage (U), Speed of advance or feed rate (S) and injection pressure or flushing pressure (P). Recycled Titanium based composite (an alloy Ti17) was used for machining operations and the combined effects of cutting parameters on the material removal MRR rate and kerf were investigated while using the analysis of variance ANOVA. Mathematical models were used for the objective of minimum kerf and maximum MRR, Cut edge surface analysis was carried out using an optic microscope and Scanning Electron Microscope (SEM) to evaluate the kerf.

Keywords WEDM · ANOVA · Taguchi method · MRR · Kerf (cutting width) · Recycled composites · Ti17

14.1 Introduction

Electrical discharge machining (EDM) an important non-conventional manufacturing method used for hard to cut conductive material and has been accepted worldwide as a standard process in the manufacture of forming tools to produce plastics mouldings, forming dies, die casting, since it does not require cutting tools and allows machining involving hard, brittle, thin and complex geometry. Wire electrical discharge machining (WEDM) is now used in automobile, aérospace and medical industries, as good as in practically all areas of conductive material machining.

WEDM is based on electric discharge machining process and it is an unconventional method of machining that includes electrically conductive materials, and involves the removal of material by the action of energy dissipated between an electrode and a workpiece. This process has kneed important progress that made it a lead of machining processes of precision and many several researchers are studied these process and their different aspects. It is the machining process during which material is eroded by series of controlled sparks between electrode and the workpiece. Workpiece and the electrode are immersed in the dielectric fluid. The area around the spark is heated to 10,000–20,000 °C and the dielectric fluid around this area is vaporized, leading to increase in the pressure. Also small amount of workpiece and electrode material melts and vaporizes, which creates small craters on the surface. A layer of melted and resolidified material called recast can be found on the surface after EDM [1–7]. I was observed from the intensive literature review that most of the studies have target the optimization of multiple quality characteristics in WEDM process such as cutting rate, wire wear rate and wire failure frequency, kerf size, Material removal rate MRR and most important quality of machined surface the surface roughness SR. Those characteristics are influenced by machining parameters. Optimization of these parameters for each material or groupe of materials is necessary [1, 9].

S. Ezeddini · M. Boujelbene · S. Ben Salem
University of Tunis El Manar, ENIT, École Nationale d'Ingénieurs de Tunis, Tunis, Tunisia

E. Bayraktar (✉)
Supmeca-Paris, School of Mechanical and Manufacturing Engineering, Saint-Ouen, Paris, France
e-mail: bayraktar@supmeca.fr

P. R. Thakre et al. (eds.), *Mechanics of Composite, Hybrid and Multifunctional Materials, Volume 5*, Conference Proceedings of the Society for Experimental Mechanics Series, https://doi.org/10.1007/978-3-319-95510-0_14

A large number of researchers have reported the optimization of multiple correlated responses of WEDM process using traditional industry. W. Tebni et al. [10] studied surface integrity by varying the parameters of EDM machining. Ozkul et al. [11] studied the influence of the machining parameters such as the pulse time On, the current I, the voltage U and the dielectric pressure and set the pause time Off. Khan and saifuddin [12] examined the wear for two copper and aluminum tools for two types of material (stainless steel and carbide), as a result of the study show that aluminum electrode was left to smother surface than copper electrode on stailess stell and carbide. Guu [13] has been worked on imaging surface on implemented electro discharge machining AISI D2 tool steel by atomic force microscopy. Prabhu and Vinayagam [14] was researched AISI D2 tool steel hardware surface features implemented electric dis-charge machining process with single wall caebon nanontubes. Observation that the surface roughness and half-cro-fractures increased proportionally with the power. Ay and Aydogdu [15] have been worked out by investigating the effects of technical parameterization on the parameters of technical parameters and their predictive values.

Present study is targeted at investigation of machining characteristics of material removal rate and kerf width in WEDM of Recycled Titanium based composite (an alloy Ti17). The outcome of this study would add to the database of the machinability of Recycled Titanium based composite (an alloy Ti17) and also would be very beneficial for the machinist as the technology charts for WEDM of this material would be updated.

14.2 Experimental Procedure

14.2.1 Equipment, Materials and Measurement

The material studied in this work is Recycled Titanium based composite (an alloy Ti17) which has been used with the chemical specification given in Table 14.1 and the chemical specification of electrode (wire) given in Fig. 14.3 and Table 14.2, a circular workpiece with a diameter of 50 mm and thikness of 3 mm was cut to 9 samples (Fig. 14.2). The experiments were carried out on a wire rod erosion machine Robofil 190. The fixed process parameters during the experiment given in Table 14.3.

Ti17 or TA5CD4 (AFNOR) is a titanium-based alloy to which the alloy elements are added (17% in all, hence its name). Like pure titanium, above a so-called β transus temperature, Ti17 has a cubic crystallographic structure centered at 100%. In contrast, unlike pure titanium hexagonal structure (h.c.) at 100% at room temperature, Ti17 is two-phase with 30% phase β (c.c.) and 70% phase α (h.c.). The structure of our material machined by WEDM is classified in the acircular structure then this structure requires only a heat treatment. It is obtained during a cooling started in the β domain and is characterized by the presence of needle in the thickness is according to the cooling rate. The structure of Widmanstatten (or basketry) produced by a slower cooling allowing the transformation of β into α. The alpha phase develops as lamellae all the thicker as the cooling rate is slower. Figure 14.1 is an example which shows the structures of Ti17 after machining with WEDM and which shows the relationship between the cooling rate and the sizes of the alpha phase lamellae. in our case we consider EDM machining as a heat treatment and the cutting speed and the dielectric pressure are proportional to the cooling rate.

14.2.2 Wire Electric Discharge Machining Process and Cutting Parameters

WEDM is currently widely used in the industry for the high-precision machining of all types of conductive materials such as metals, metal alloys, graphite or even certain ceramic materials of any hardness, WEDM is used in a wide range of industries, including aerospace, biomedical, automotive, as well as molds. In this study, we are interested in the recycled Titanium based

Table 14.1 Chemical composition

Element	Ti	Al	Mo	Cr	Zr	Sn	O
%	83	5	4	4	1.9	2	0.1

Table 14.2 Chemical composition of wire tool

Composition of wire	Mass%	Atom%
Cuivre-Cu	57.59	58.28
Zinc-Zn	42.41	41.72

Table 14.3 Fixed parameters

Wire	Brass wire of diameter 0.25 mm
Shape and size of work piece	Circular piece of diameter 50 mm and thickness 3 mm
Dielectric fluid	Deionized water

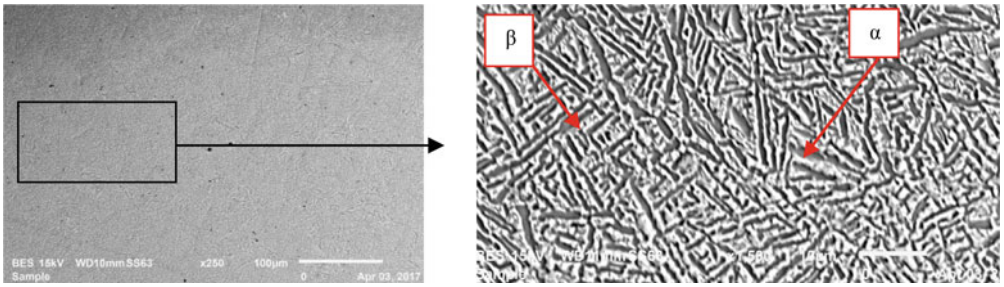

Fig. 14.1 Microstructure of Ti17 after WEDM machining (S (mm/min) =36, P (bar) =80)

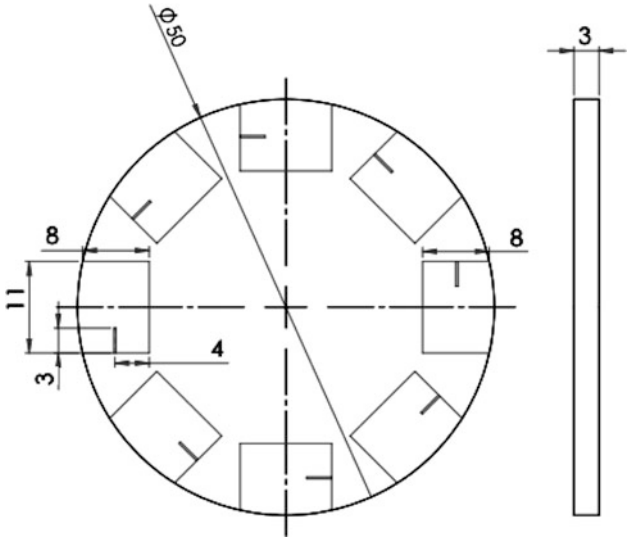

Fig. 14.2 Experimental configuration for work-piece

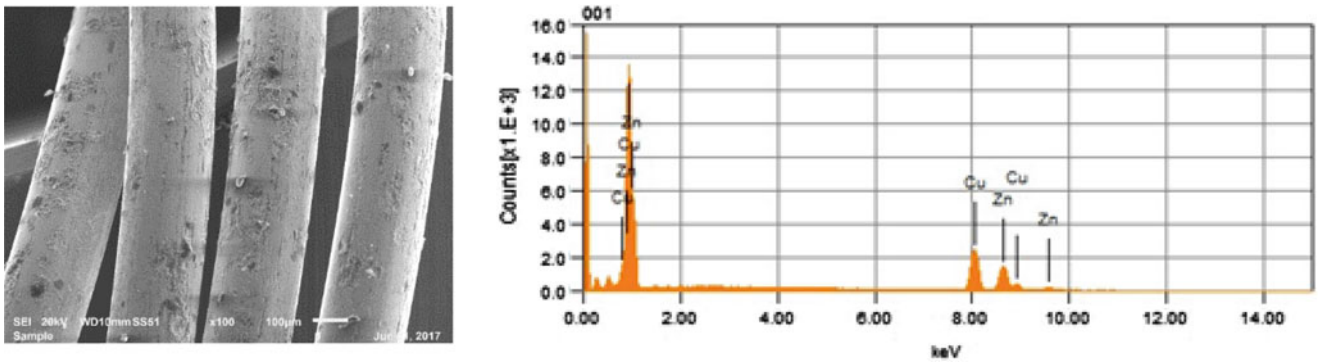

Fig. 14.3 SEM picture of wire tool and composition of wire tool from SEM analysis

composite (an alloy Ti17 which are known to be the most difficult materials to machine, so tests of cutting by the machine of the wire EDM were carried out on the material. In order to optimize this method, an integrated method was used which brings together the Taguchi method and the RSM response surface methodology (Figs. 14.2 and 14.3).

Table 14.4 The basic Taguchi L9 (3^4) orthogonal array

	Control factors and levels				Coding				Results	
Run	U(V)	Ton(µs)	S(mm/min)	P(bar)	X1	X2	X3	X4	Kerf(µm)	MRR (µm)
1	80	0.8	29	60	−1	−1	−1	−1	341.83	39.65
2	80	0.9	36	80	−1	0	0	0	341.36	49.116
3	80	1	43	100	−1	1	1	1	346.83	59.654
4	100	0.8	36	100	0	−1	0	1	345.07	49.690
5	100	0.9	43	60	0	0	1	−1	341.06	58.662
6	100	1	29	80	0	1	−1	0	331.86	38.495
7	120	0.8	43	80	1	−1	1	0	309.88	53.299
8	120	0.9	29	100	1	0	−1	1	317.78	36.862
9	120	1	36	60	1	1	0	−1	317.03	45.652

Table 14.5 Attribution of the levels to the factors

	Pulse on time Ton(µs)	Servo voltage U(V)	Speed of advance S (mm/min)	Flushing pressure P(bar)
Levels	T	U	S	P
1	0.8	80	29	60
2	0.9	100	36	80
3	1	120	43	100

In this work we used The Taguchi method and the Response Surfaces Methodology (RSM) to efficiently analyze the experimental data and seek satisfactory solutions. First, the Taguchi method is used to collect experimental data and to study in a preliminary way the link between the objectives and the parameters. In this case, the RSM models are designed to approximate the target functions, so that a multi-objective model is easy to acquire.

The standard experimental model based on Taguchi an orthogonal matrix L 9 (3^4) was used in this study and presented in Table 14.4. This basic design uses up to four control factors, with three levels each. A total of nine experimental runs must be performed, using the combination of levels for each control factor as shown in Table 14.5. Four control factors including pulse (Ton), startup voltage (U), feed rate or speed advance (S) and flushing pressure (P) for kerf width and material removal rate MRR have been selected.

Taguchi method is statistical method, or sometimes called robust design method, developed by Genichi Taguchi to improve the quality of manufactured goods, to evaluate losses due to poor quality and to seek to minimize noise sensitivity for any product and / or process, and more recently also applied to engineering, biotechnology and marketing. The application of this technique has become widespread in many American and European industries after the 1980s. The advantage of Taguchi design is the study of multiple factors can be considered at once. Therefore, not only the controlled factors can be considered, but also noise factors for example. Although similar to experimental design (DOE), the Taguchi design or method only leads to balanced (orthogonal) experimental combinations, making the Taguchi design even more efficient than a fractional factor design. By using Taguchi techniques, industries are able to dramatically reduce the development cycle time of the product for design and production, improve manufacturing efficiency and performance reliability, thereby reducing costs and increasing profits. In addition, the Taguchi design allows us to examine the variability caused by noise factors, which are generally ignored in the traditional DOE approach. The Taguchi method requires only a smaller number of orthogonal experimental combinations that dramatically improve design efficiency. There are several researchers who have used the Taguchi method (Farnaz Nourbakhsh et al. (2013) [16] is a study where they used a Taguchi L18 plane to optimize input parameters (current, pulse time, Tension and wire tension) to improve surface integrity, Boujelbene et al. [21] have done an optimization of MRR material removal rate, TWR wire wear rate and surface roughness using the L25. Two basic tools in the Taguchi technique are the orthogonal network (OA) and the signal-to-noise ratio (S/N). OA is used in the Taguchi method to save time and cost experiments. The S/N ratio is used to measure the deviation of the quality characteristics from the desired values, including the highest Higher-The-Better (HTB), Nominal-The-Better (NTB) and Lower-The-Better LTB). In [17] they studied the variation of kerf and rate of removal of MRD WEDM materials by using ANOVA and SN ration. In this study we aim to optimize the kerf and the material removal rate MRR so that the most objective type of objective function is High-The-Better) And Lower-The-Better (STB) were used. The exact relationship between the S/N ratio and the signal is given by the following Eqs. (14.1) and (14.2):

HTB: Eq. (14.1); LTB: Eq. (14.2)

$$\frac{S}{N} = -10 * \log\left(\sum_{i=0}^{n} Yi^2/n\right) \tag{14.1}$$

$$\frac{S}{N} = -10 * \log\left(\sum_{i=0}^{n} \left(1/Yi^2\right)/n\right) \tag{14.2}$$

Where n is the number of experiments, and y_i is the value of the kerf or MRR.

The Response Surface Method (RSM) proposed by Box and Wilson (1951) in the early 1950s received considerable attention because of its good empirical performance in modeling. It is a set of mathematical and statistical techniques that provide adapted models between input parameters and responses to develop improve and optimize a process. Several researches have used the RSM method to improve and optimize the performance of machining processes such as surface integrity (roughness, heat affected zone, residual stress), MRR material removal rate, thread wear TWR, kerf [19–20]. The most extensive application of RSM is found in the industrial world, especially in the case where several input variables potentially influence the performance measures or the product or process quality characteristics [18]. This study seeks an appropriate approximation method for analyzing the surface roughness relationship Ra, the thermally affected zone HAZ with respect to independent input parameters. A mathematical equation of the second order polynomial response surface is used as indicated in the equation; the coefficients of the function can be obtained by the least squares method

$$Y = \beta_0 + \sum_{i}^{n} \beta_i X_i + \sum_{i<j}^{n} \sum \beta_{ij} X_i X_j + \sum \beta_{ij} X_i^2 + \varepsilon \tag{14.3}$$

Where y denotes kerf or MRR, x represents the parameters of WEDM (T_{on}: pulse time, U: start up voltage or servo voltage, S: feed rate or speed advance and P: flushing pressure or dielectric injection pressure), B_{ij} is the coefficients of each term, ε is a residual error. Table 14.3 shows the basic Taguchi L9 orthogonal array.

14.2.3 Influence of Machining Parameters on Performance of WEDM Process

14.2.3.1 Influence of Machining Parameters on Kerf Width

The Kerf is defined as the width of the piece that is removed by a cutting process. When you cut parts on a CNC machine, you would make precision cuts with finished dimensions as close as possible to the programmed shape. This drives us to study the kerf and to look for how we can act on this performance from the machining conditions. Thus gap is determined by the intensity of the spark energy. Figure 14.4 shows the different slots effected by wire of electric discharge machine whie machining of Ti17 alloy. Their slots are machined by differents machining conditions.

Figure 14.5 shows the effect of flushing pressure on the kerf width in three values of servo voltage U = 80 V, U = 100 V, and U = 120 V, in three cases kerf width has the same trend, it decrease with increase of flushing pressure from 60 bar to 80 bar after that it increase.

Figure 14.6 shows the effect of advance speed on the kerf width in tow values of servo voltage U = 100 V and U = 120 V, from this figure kerf widh knew a little increasing winth increase of advanced speed with servo voltage U = 100 V.

Kerf width presented a constant profile us function a pulse on time (Ton) with tow different values of servo voltage U = 80 V and U = 120 V, it is mean that pulse on time don't have a great influence on the kerf width see Fig. 14.7. In the other hand, Fig. 14.8 showed the great influence of servo velotage (U) then, the kerf width decreases with the increase of servo voltage.

14.2.3.2 Influence of Machining Parameters on Material Removal Rate MRR

Material removal machining is a process for manufacturing mechanical parts.

Remove material to give the raw piece the desired shape and size, using a machine tool. By this technique, we obtains a parts with great precision.

This processing method makes it possible to manufacture parts with very complex geometry and small gaps or small internal rays. We obtain surfaces of extreme finesse and precision.

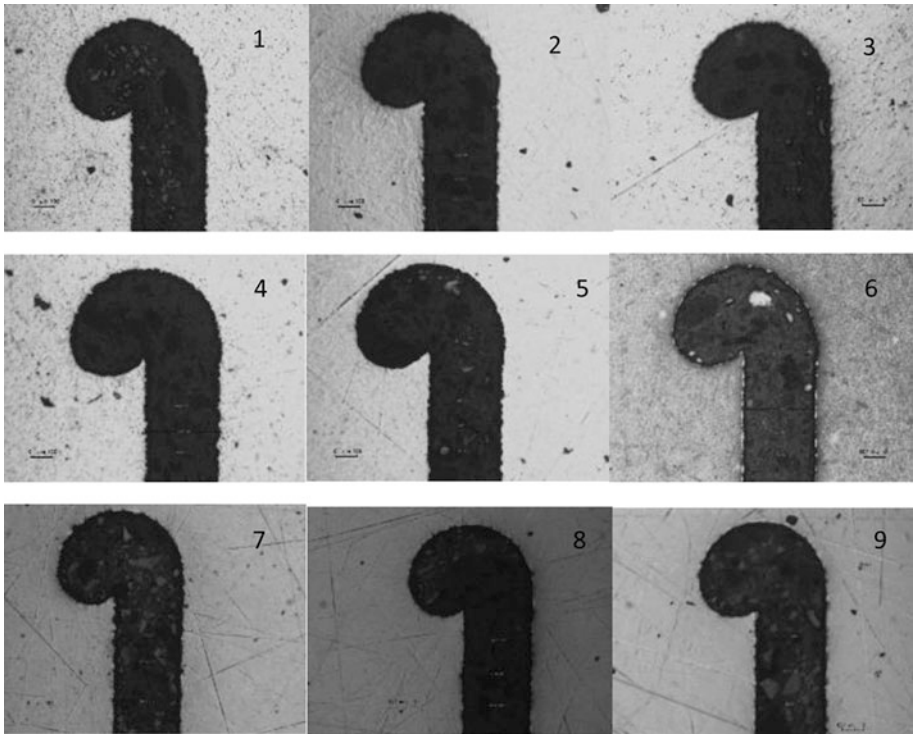

Fig. 14.4 Kerf width for 9 different samples

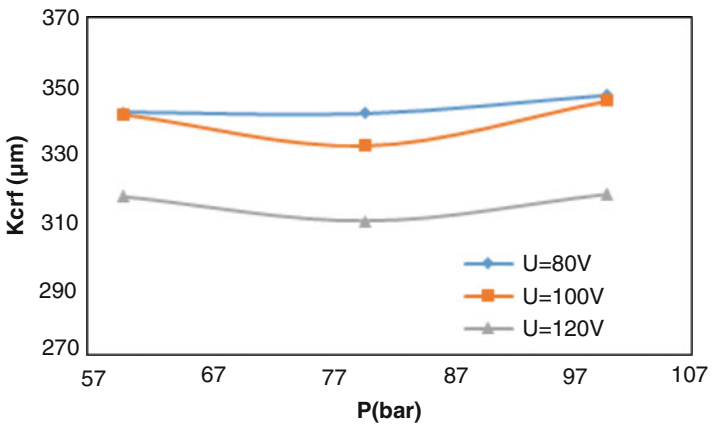

Fig. 14.5 Effect of flushing pressure P on kerf width

To measure the removal rate of material MRR from wire EDM machining of the aluminum titanium based MRR intermetallic composite; a slit at the edge of the sample was made as shown in Fig. 14.9 to calculate the MRR of each sample with Eq. (14.4).

$$MRR = S^* e^* p \tag{14.4}$$

S = advance speed mm/min
e = thickness of the workpiece in mm
p: Depth of the slot made by the wire in mm

Figures 14.10, 14.11, 14.12, and 14.13 show the evolution of material removal rate according to the WEDM machining parameters during the machining of Ti17 alloy. From curves in Fig. 14.12 we notice that MRR increases with a big pent with the increase of advanced speed or feed rate (S) with the two differents values of flushing pressure. In other hand MRR

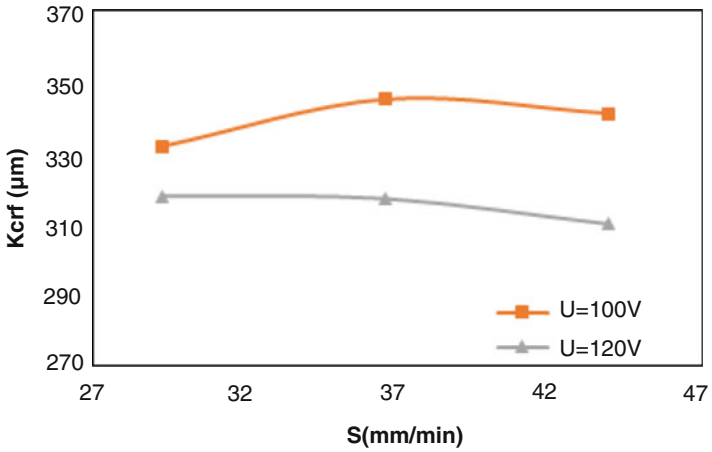

Fig. 14.6 Effect of advance speed on kerf width

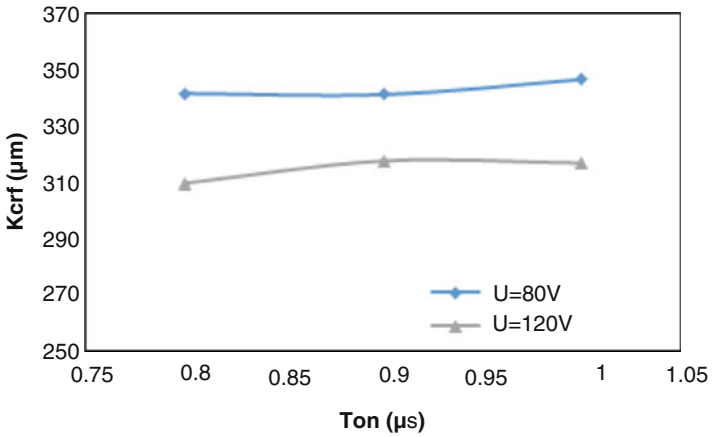

Fig. 14.7 Effect of pulse on time Ton on kerf width

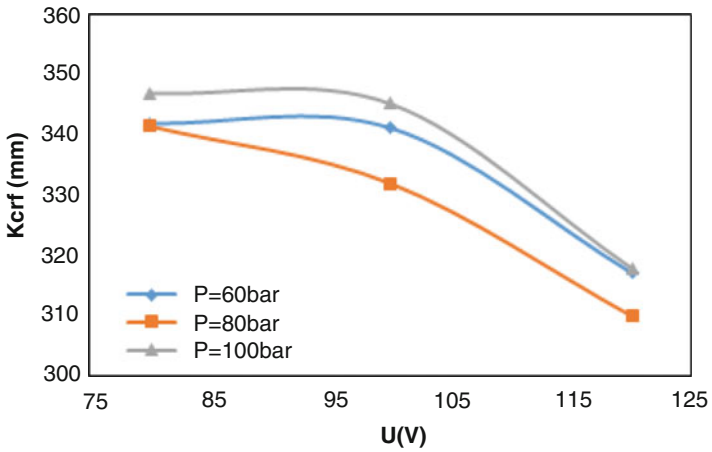

Fig. 14.8 Effect of servo voltage U on kerf width

decreases a very little with increase of servo voltage (Fig. 14.10) and increases a very little with increase of flushing pressure (Fig. 14.13).

The surface topographical images of microchannels fabricated by WEDM in recycled Titanium based composite (an alloy Ti17) material are shown in Fig. 14.14. The effects of machining parameters of cutting on channel width are shown

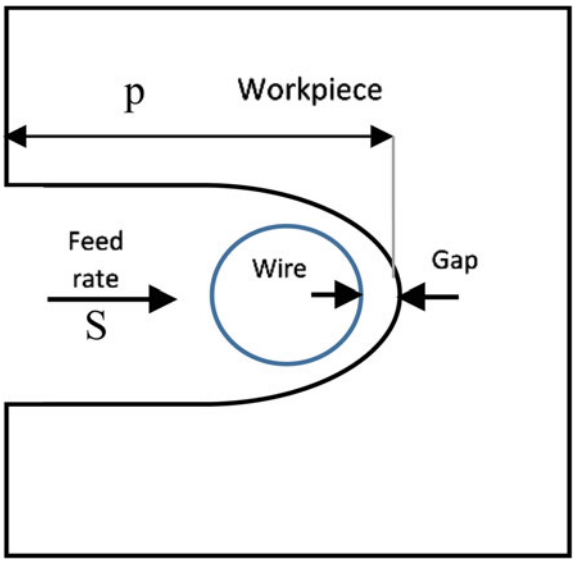

Fig. 14.9 Kerf width

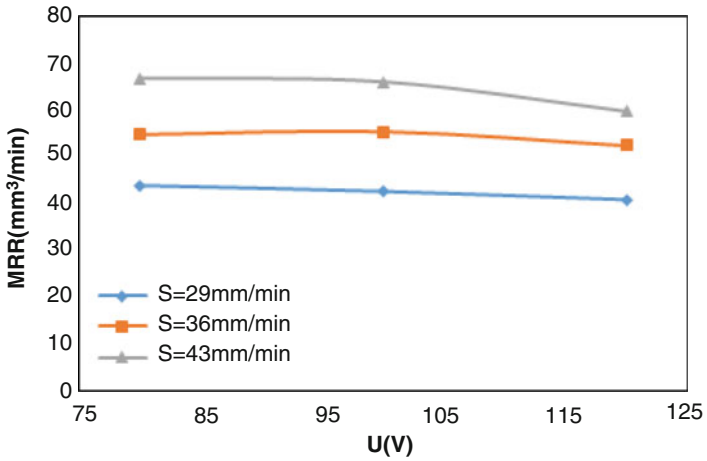

Fig. 14.10 Effect of servo voltage on MRR

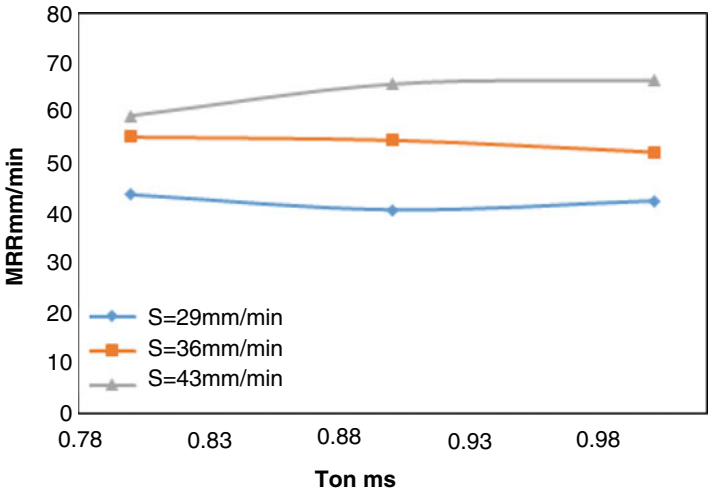

Fig. 14.11 Effect of pulse on time on MRR

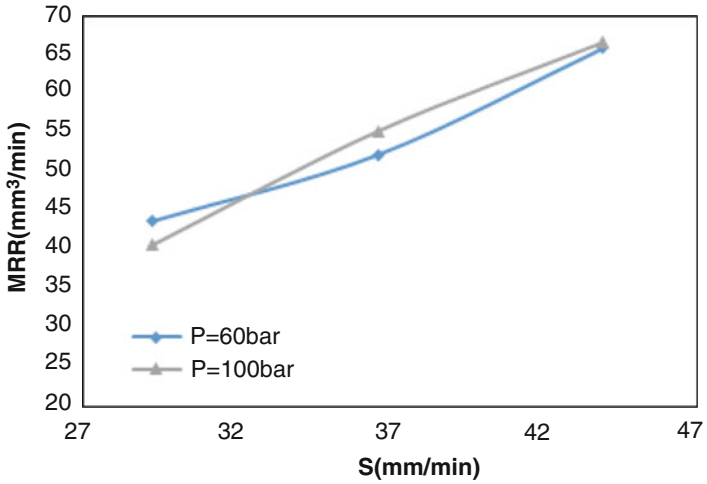

Fig. 14.12 Effect of advance speed on MRR

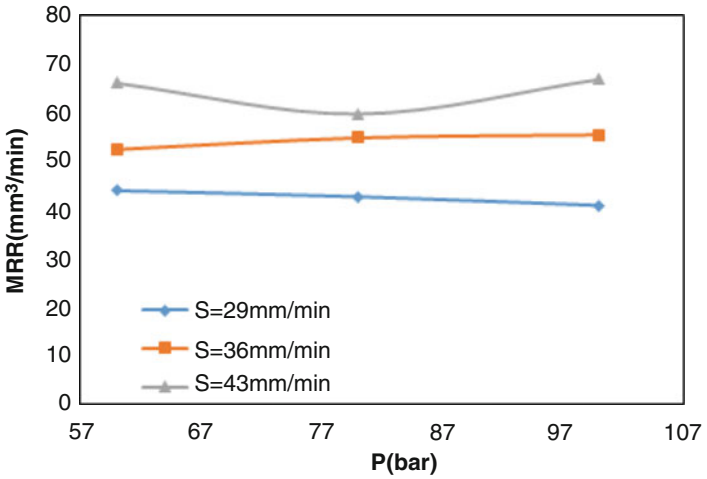

Fig. 14.13 Effect of flushing pressure on MRR

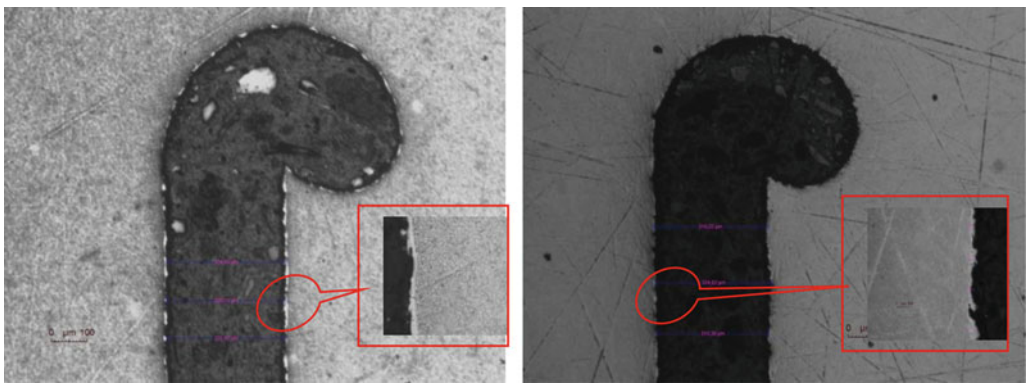

Fig. 14.14 optic picture in the internal surface of the Ti17 alloy Kerfs machined by WEDM with: (**a**) U = 100 V, Ton = 1 μs, S = 29 mm/min, P = 80bars; (**b**) U = 120 V, Ton = 0.9 μs, S = 29 mm/min, P = 100bars

in Fig. 14.14a, b, we observe a big variation on the surface and subsurface and the presence of the "white ayer", because WEDM process uses heat from electrical sparks to cut the material, the spark creat a heat affected zone that contains a thin layer of recast called'White layer" like in the Fig. 14.14 and the depth of the heat affected zone and recast depends of energy and power.

Table 14.6 Response table for signal to noise ratios smaller is better and for means of kerf

	Level	Means				S/N ratio			
Process parameters		U(V)	Ton(μs)	S(mm/min)	P(bar)	U(V)	Ton(μs)	S(mm/min)	P(bar)
Average value	L1	343.3	332.3	330.5	333.3	−50.71	−50.42	−50.38	−50.45
	L2	339.3	333.4	334.5	327.7	−50.61	−50.45	−50.48	−50.30
	L3	314.9	331.9	332.6	336.6	−49.96	−50.41	−50.43	−50.53
	Delta	28.4	1.5	4.0	8.9	0.75	0.04	0.10	0.23
	Rank	1	4	3	2	1	4	3	2

Table 14.7 Response table for signal to noise ratios larger is better and for means of MRR

		Means				S/N ratio			
Process parameters	Level	U(V)	Ton(μs)	S(mm/min)	P(bar)	U(V)	Ton(μs)	S(mm/min)	P(bar)
Average value	L1	49.48	47.55	38.34	47.99	33.77	33.48	31.67	33.51
	L2	48.95	48.21	48.15	46.97	33.67	33.51	33.65	33.36
	L3	45.27	47.93	57.21	48.74	33.02	33.47	35.14	33.59
	Delta	4.20	0.67	18.87	1.76	0.75	0.04	3.47	0.23
	Rank	2	4	1	3	2	4	1	3

Table 14.8 S/N ratio means and predicted S/N ratio and predicted means of Kerf

	Control factors and levels				Results					
Run	U(V)	Ton(μs)	S(mm/min)	P(bar)	kerf	Pred kerf	SNRA	MEAN	PMEAN	PSNRA
1	80	0.8	29	60	341.83	341.83	*50.6763*	*341.833*	*341.833*	*−50.6763*
2	80	0.9	36	80	341.36	341.362	*−50.6645*	*341.367*	*341.367*	*−50.6645*
3	80	1	43	100	346.83	346.83	*−50.8024*	*346.830*	*346.830*	*−50.8024*
4	100	0.8	36	100	345.07	345.07	*−50.7582*	*345.070*	*345.070*	*−50.7582*
5	100	0.9	43	60	341.06	341.06	*−50.6566*	*341.060*	*341.060*	*−50.6566*
6	100	1	29	80	331.86	331.86	*−50.4191*	*331.860*	*331.860*	*−50.4191*
7	120	0.8	43	80	309.88	309.88	*−49.8239*	*309.880*	*309.880*	*−49.8239*
8	120	0.9	29	100	317.78	317.78	*−50.0425*	*317.780*	*317.780*	*−50.0425*
9	120	1	36	60	317.03	317.03	*−50.0220*	*317.030*	*317.030*	*−50.0220*

14.3 Statistical Analysis

Tables 14.6 and 14.7 show response table for means and signal to noise ratio for kerf and MRR of Recycled Titanium based composite (an alloy Ti17) material successive. This response table represents the effects of various input factors on kerf and MRR. Higher the slope in the main effects plot corresponding values of delta is higher in the response table. The rank represents directly the level of effect of input based on the values of delta. Here according to ranks, the effects of various input factors on kerf in sequence of its effect are servo voltage and flushing pressure and the effects of various input factors on MRR in sequence of its effect are advanced speed and servo voltage. That means servo voltage affects the kerf at highest level and at lowest level. And advanced speed affects MRR at highest level and lowest level.

Tables 14.8 and 14.9 shows the values of signal to noise ratio (SNRA) and Predicted signal to noise ratio (PSNRA) for kerf and MRR of recycled Titanium based composite (an alloy Ti17) material successive. The values of predicted signal to noise is very much close to the calculated signal to noise values hence the analysis of Taguchi for signal to noise ratio is correct, it's perfect. The representation of effects of various parameters on kerf and MRR and optimize condition is very much nearby.

Figures 14.14 and 14.15 show the influence of each cutting parameter: the pulse on time, the servo voltage, the feed rate or advanced speed and the injection pressure or flushing pressure. However, according to the curves of the effects (Fig. 14.14), the servo voltage has the greatest influence on the kerf values and the value U = 120 V corresponds to the smallest kerf value compared with U1 and U2. In addition, the speed S1 corresponds to the smallest kerf value with compared with S3 and S2, the pulse time $T_{on}3$ corresponds to the smallest kerf value compared with $T_{on}1$ and $T_{on}2$ and the flushing prssure P2 corresponds to the smallest kerf value compared with P1 and P3. In other hand, according to the curves of the effects (Fig. 14.15), the advanced speed has the greatest influence on the MRR values and the value S 3 = 43 mm/min corresponds to the

Table 14.9 S/N ratio means and predicted S/N ratio and predicted means of MRR

	Control factors and levels				Results					
Run	U(V)	Ton(μs)	S(mm/min)	P(bar)	Ra	Pred Ra	SNRA	MEAN	PMEAN	PSNRA
1	80	0.8	29	60	2.92	2.9288	31.9653	39.6527	39.6527	31.9653
2	80	0.9	36	80	1.93	1.9475	33.8247	49.1184	49.1184	33.8247
3	80	1	43	100	1.74	1.7400	35.5128	59.6548	59.6548	35.5128
4	100	0.8	36	100	1.96	1.9425	33.9253	49.6901	49.6901	33.9253
5	100	0.9	43	60	2.48	2.4713	35.3671	58.6623	58.6623	35.3671
6	100	1	29	80	2.01	1.9838	31.7081	38.4958	38.4958	31.7081
7	120	0.8	43	80	2.48	1.8487	34.5344	53.2994	53.2994	34.5344
8	120	0.9	29	100	1.8	1.8175	31.3316	36.8625	36.8625	31.3316
9	120	1	36	60	2.84	2.8400	33.1892	45.6523	45.6523	33.1892

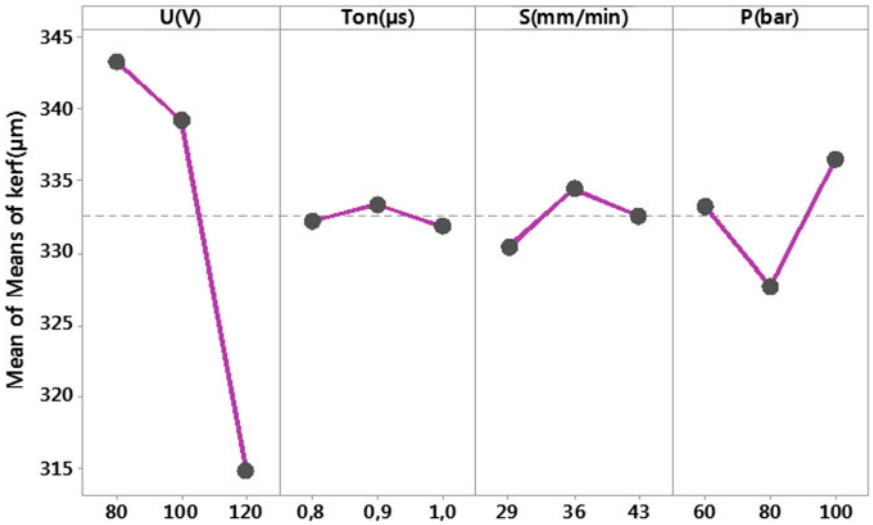

Fig. 14.15 The effect of machining parameters on kerf (μm)

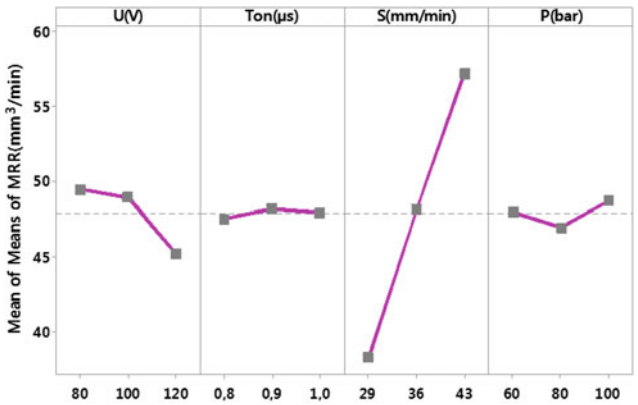

Fig. 14.16 The effect of machining parameters on MRR

bigest MRR value compared with S1 and S2 the servo voltage U1 corresponds to the greast MRR value wcompared with U3 and U2, the flushing pressure P2 corresponds to the biggest MRR value compared with P1 and P2.

The S/N ratio was used to determine the optimum parameters for a smaller value of kerf in WEDM machined surface of Ti17 alloy and according to Fig. 14.16 and Table 14.6 the optimal level of the machining parameters is the level with the greatest S/N ratio.

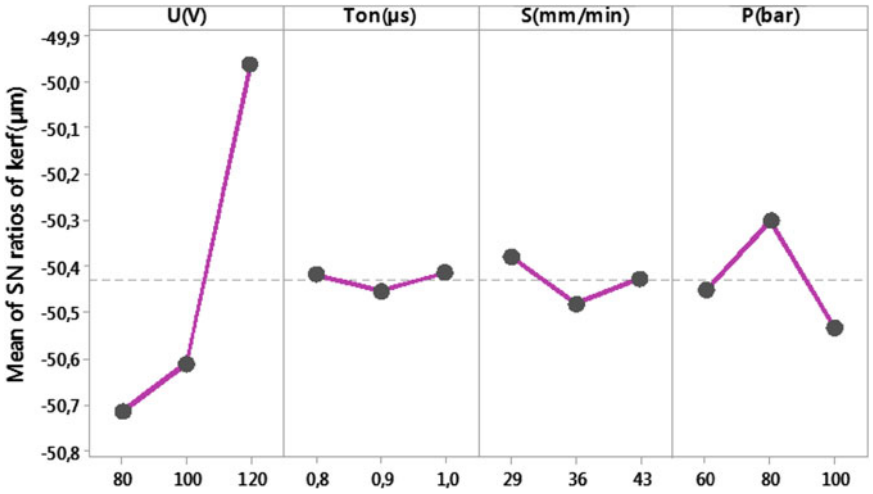

Fig. 14.17 Main effects plot for SN ratios for kerf

Table 14.10 ANOVA result for Kerf

Source	DF	Seq SS	Cont%	Adj SS	Adj MS	F-Value	P-Value	Remarks
Model	8	4711.27	99.60%	4711.27	588.909	555.19	0.000	Significant
U(V)	1	3641.46	76.98%	461.80	461.799	435.36	0.000	Significant
T_{on}(µs)	1	0.57	0.01%	10.26	10.262	9.67	0.006	–
S (mm/min)	1	19.82	0.42%	55.65	55.653	52.47	0.000	Significant
P (bar)	1	47.60	1.01%	294.85	294.855	277.97	0.000	Significant
U^2 (V)	1	625.46	13.22%	625.46	625.465	589.65	0.006	–
Ton^2(µs)	1	10.43	0.22%	10.43	10.428	9.83	0.000	Significant
S^2	1	52.16	1.10%	52.16	52.156	49.17	0.000	Significant
P^2(bar)	1	313.78	6.63%	313.78	313.782	295.81	0.000	Significant
Error	18	19.09	0.40%	19.09	1061			
Total	26	4730.37	100.00%					
S			R-sq		R-sq(adj)		R-sq(pred)	
1.02992			99.60%		99.42%		99.09%	

In Fig. 14.17 The S/N ratio was used to determine the optimum parameters for a great value of MRR in WEDM machined surface of Ti17 alloy and according to Fig. 14.17 and Table 14.7 the optimal level of the machining parameters is the level with the greatest S/N ratio.

Analysis of variance (ANOVA) is used to evaluate the model developed, as shown in Tables 14.10 and 14.11, analysis of the ANOVA variance is a result which makes it possible to see if the variables Explanations give significant information to the model or not.

Larger F-Value indicates that the variation of the process parameter makes a big change on the performance characteristics. F-Values of the machining parameters are compared with the appropriate confidence table.

According to F_{test} analysis the significant parameters on the kerf *are* flushing pressure P, servo voltage U, feed rate S and P^2, T^2 and S^2, in addition on the MRR all parameters are significants. The percent contributions on the machining parameters on the kerf and MRR are shown in Tables 14.7 and 14.8.

Equations 14.5 and 14.6 presented the regression Equation of ker and MRR models:

$$Kerf\ (\mu m) = 73,9 + 4,394 \times U + 235,5T_{on} + 4,482 \times S - 2,811 \times P - 0,02553 \times U^2 - 131,8 \times {T_{on}}^2 - 0,06017 \times S^2 + 0,01808 \times P^2 \quad (14.5)$$

Table 14.11 ANOVA result for MRR

Source	DF	Seq SS	Cont%	Adj SS	Adj MS	F-Value	P-Value	Remarks
Model	8	1713.54	99.97%	1713.54	214.193	8899.64	0.000	Significant
U(V)	1	79.53	4.64%	11.16	11.156	463.54	0.000	Significant
T_{on}(μs)	1	0.67	0.04%	1.41	1.406	58.42	0.000	Significant
S (mm/min)	1	1602.09	93.47%	10.10	10.102	419.73	0.000	Significant
P (bar)	1	2.51	0.15%	10.79	10.791	448.38	0.000	Significant
U^2 (V)	1	14.90	0.87%	14.90	14.90	619.24	0.000	Significant
Ton^2(μs)	1	1.35	0.08%	1.35	1.35	55.91	0.000	Significant
S^2	1	0.88	0.05%	0.88	0.88	36.45	0.000	Significant
P^2(bar)	1	11.61	0.68%	11.61	11.61	482.54	0.00	Significant
Error	18	0.43	0.03%	0.43	0.024		0.00	Significant
Total	26	1713.98	100%					
S			R-sq		R-sq(adj)		R-sq(pred)	
0.155137			99.97%		99.96%		99.94%	

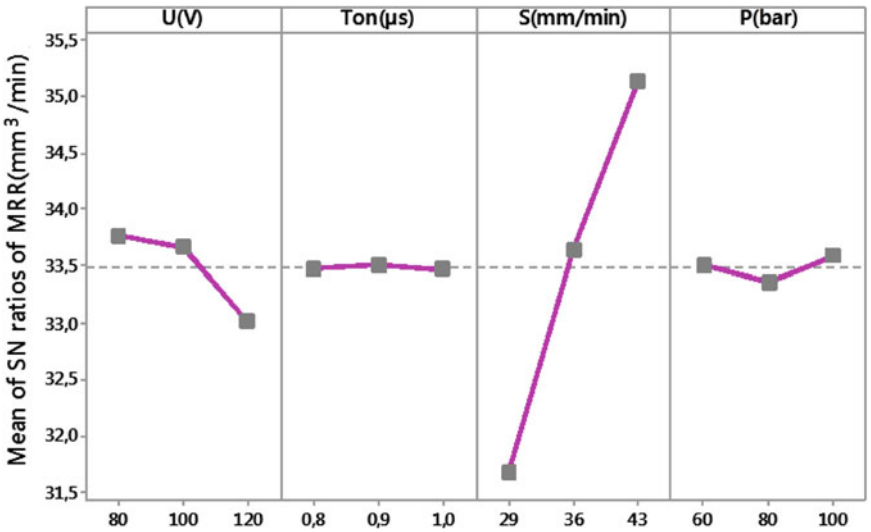

Fig. 14.18 Main effects plot for SN ratios for MRR

$$\begin{aligned} \text{MRR}\,(\mu m) = &-58,27 + 0,6829 \times U + 87,2 \times T_{on} + 1,9096 \times S - 0,5378 \times P - 0,003940 \\ &\times U^2 - 47,36 \times {T_{on}}^2 - 0,00780 \times S^2 + 0,003478 \times P^2 \end{aligned} \tag{14.6}$$

Figures 14.18 and 14.19 show that the residuals are distributed approximately in a straight line, showing a good relationship between the experimental and predicted values for all *Kerf* performances, and MRR, and the variable follows the normal distribution. Therefore, the developed models (Eqs. 14.5 and 14.6) are considered to be fairly adapted to the observed values. Likewise, these figures show that the residues found are randomly dispersed but are independent.

Figures 14.20 and 14.21 shows the effect of servo voltage and flushing pressure P on kerf, and the effects of advanced speed and servo voltage on MRR. As is clear, smaller values of kerf can be obtained by selecting greater servo voltage. In other hand, greater values of MRR can be obtained by slecting great advanced speed. s

The RSM models are carried out with 9 experimental tests and on evry sample we affected three test of kerf value and MRR value. For each combination of the input factors, the prediction value of the response $Y_{j,pred}$ is compared with the experimental value of the response $Y_{j,exp}$. Figures 14.21 and 14.22 illustrate the comparison between the experimental and predictive response values, comparing predictive and experimental value of kerf and comparing predictive and experimental value of MRR, to test the interpolation of the prediction of the models developed by RSM (Eqs. 14.5 and 14.6). We conclude that the predictive results with RSM are very close to the experimental results (Figs. 14.23 and 14.24).

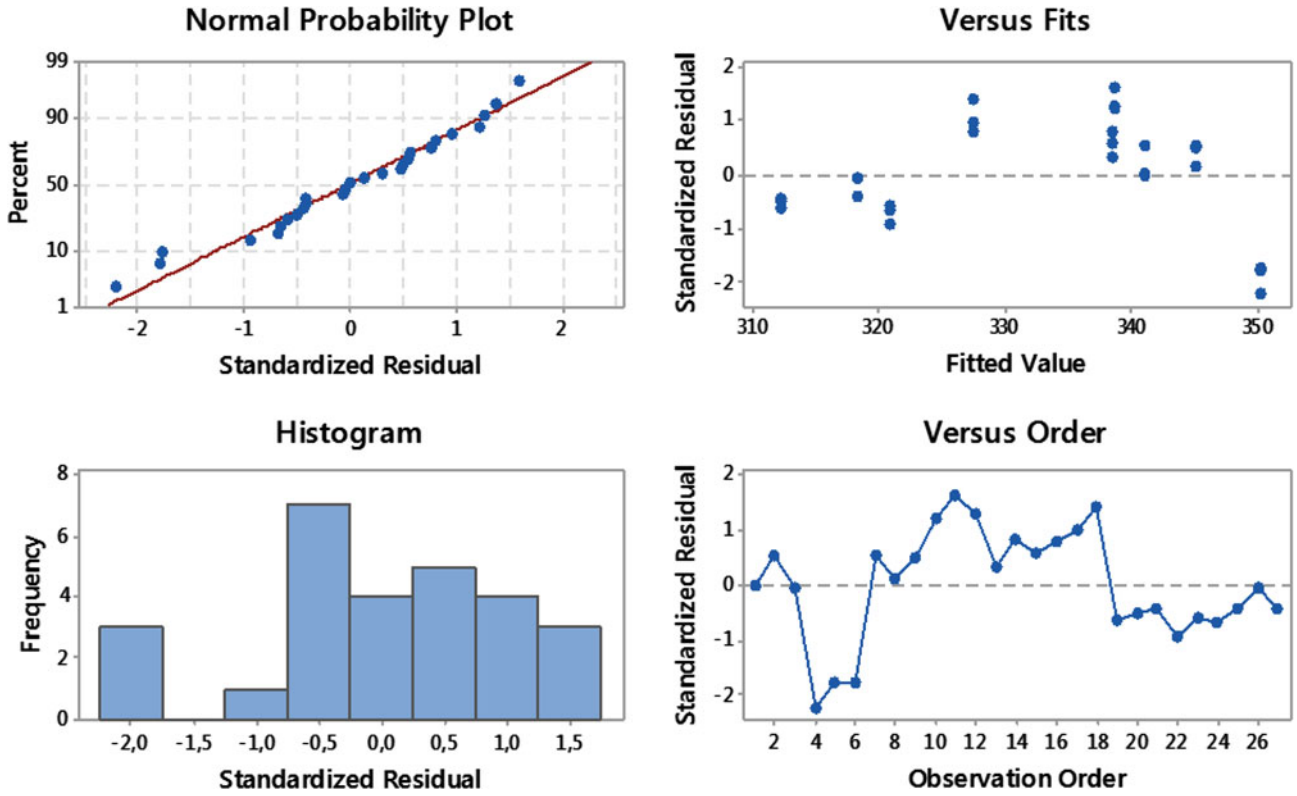

Fig. 14.19 Residual plots for Kerf

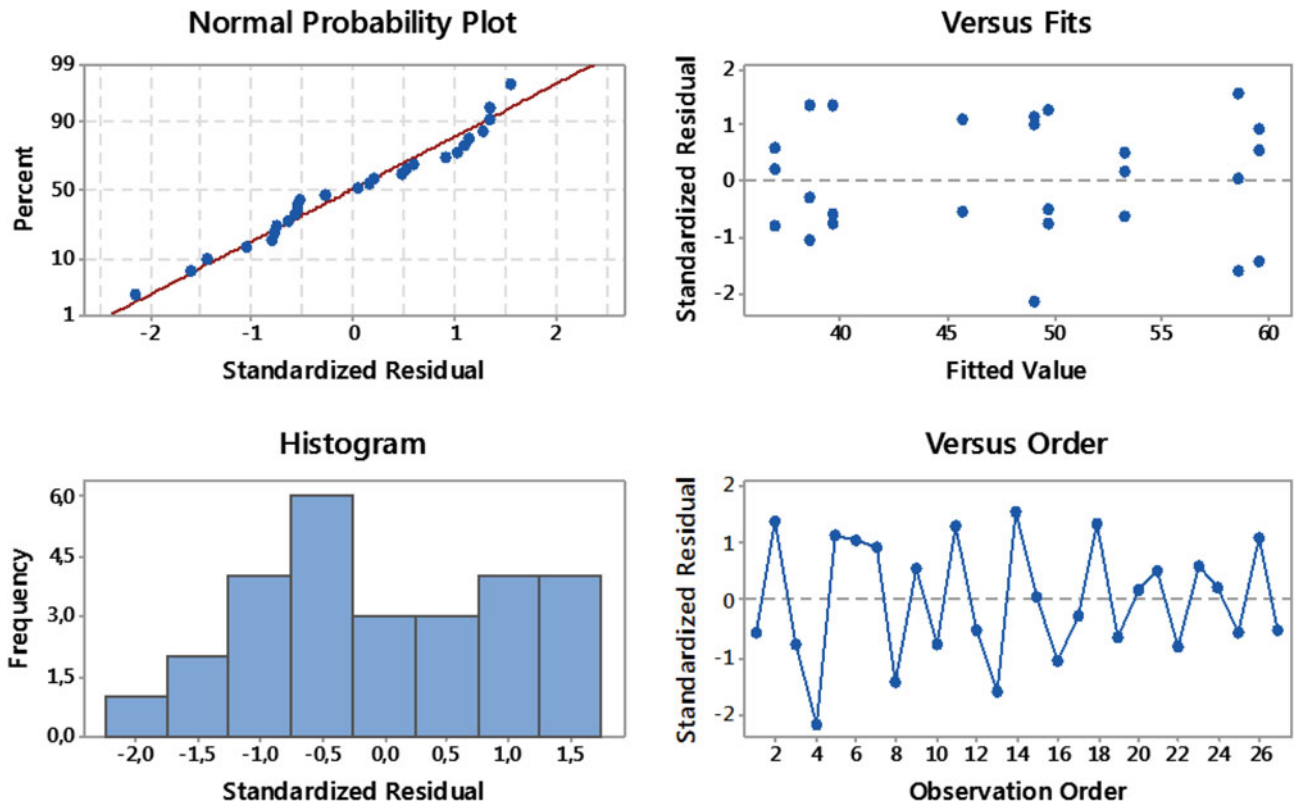

Fig. 14.20 Residual plots for MRR

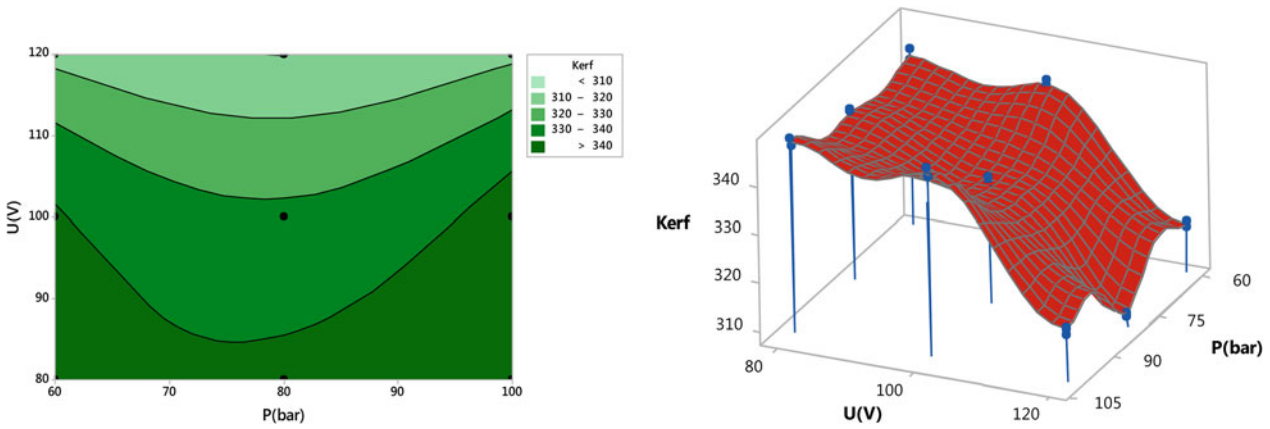

Fig. 14.21 Contour and 3D plots for kerf as function servo voltage and flushing pressure

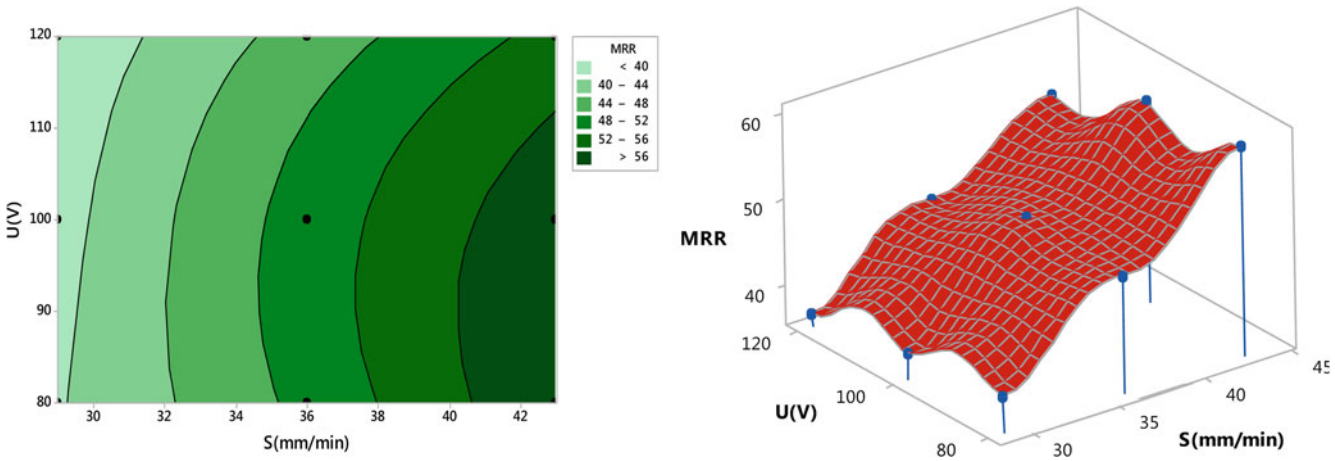

Fig. 14.22 Contour and 3D plots for MRR as function advance speed S and servo voltage

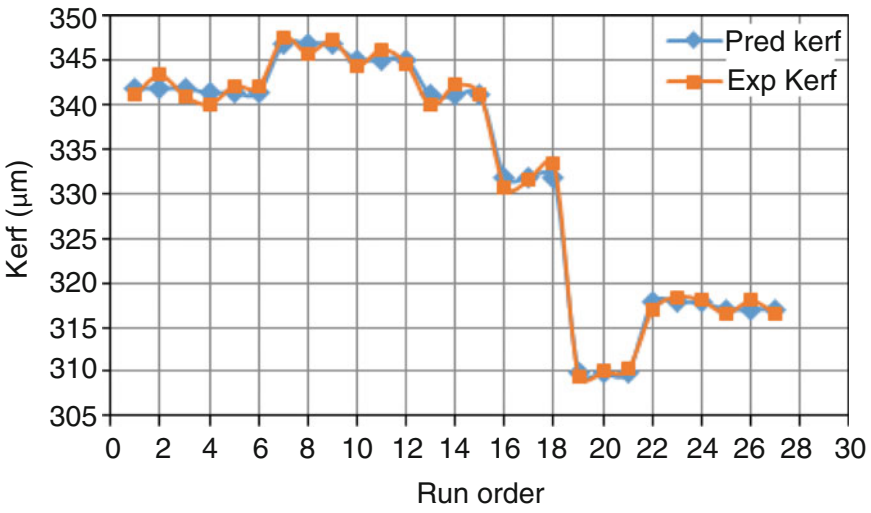

Fig. 14.23 Comparison between measured and predicted values for surface roughness Ra

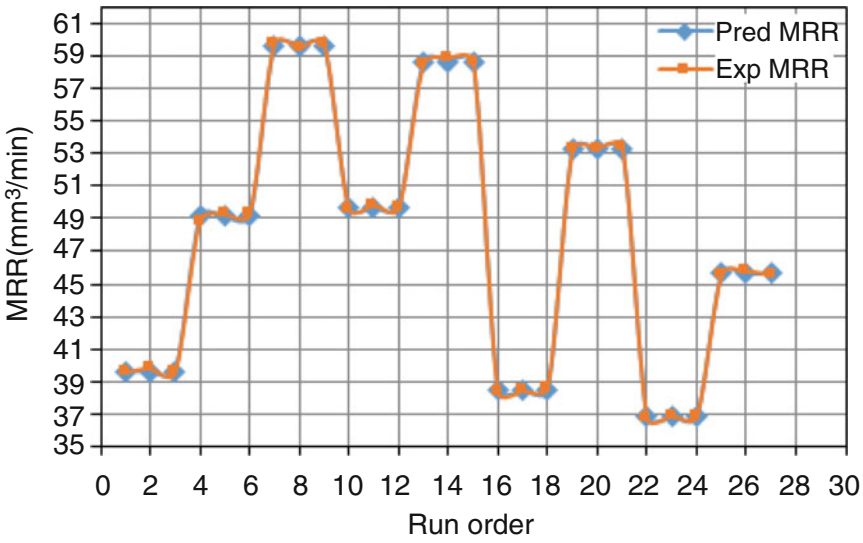

Fig. 14.24 Comparison between measured and predicted values for surface roughness Ra

14.4 Conclusions

In this paper, the application of RSM on the WEDM of v to obtain mathematical model for both the kerf width and the material removal rate MRR while investigating the influences of machining parameters optimum values of machining parameters have been studied and computed. The foremost conclusions which can be draw are as follows:

- All the input parameters considered for the experimental investigation were found to be statistically significant for their effects on the kerf and MRR.
- Smaller values of kerf can be obtained by selecting greater servo voltage. In other hand, greater values of MRR can be obtained by selecting great advanced speed.
- the servo voltage has the greatest influence on the kerf values and the value U = 120 V corresponds to the smallest kerf value compared with U1 and U2
- the advanced speed has the greatest influence on the MRR values and the value S 3 = 43 mm/min corresponds to the bigest MRR value compared with S1 and S2
- The values of predicted signal to noise is very much close to the calculated signal to noise values hence the analysis of Taguchi for signal to noise ratio is correct, it's perfect. The representation of effects of various parameters on kerf and MRR and optimize condition is very much nearby.

References

1. Mouralova, K., Kovar, J., Klakurkova, L., Prokes, T., Horynova, M.: Comparison of morphology and topography of surface of WEDM machined structural materials. Measeurement. **104(** 12–20 (2017)
2. Knight, W.A., Boothroyd, G.: Fundamentals of Metal Machining and Machine Tools, 3rd edn. CRC Press (2005). Roca Baton, Florida, USA, ISBN 1574446592
3. Jain, V.K.: Advanced Machining Process. Allied Publishers, Ballard Estate, Mumbai, India (2009)
4. E.C. Jameson. Electrical Discharge Machining, 2001., ISBN08-726-3521-X
5. Tai, T.Y., Lu, S.J.: Improving the fatigue life of electro-discharge. Machined SDK1111 tool steel via the suppression of surface cracks. Int. J. Fatigue. **31**(3), 433–438 (2009)
6. Lee, S.H., Li, X.: Study of the surface integrity of the machined workpiece in the EDM of tungsten carbide. J. Mater. Process. Technol. **139**(1), 315–321 (2003)
7. Zeid, O.A.: On the effect of electro discharge machining parameters on the fatigue life on AISID6 tool steel. J. Mater. Process. Technol. **68**(1), 27–32 (1997)
8. Chalisgaonkar, R., Kumar, J.: Multi-response optimization and modeling of trim cut WEDM operation of commercially pure titanium (CPTi) considering multiple user's performances. Eng. Sci. Technol. Int. J. **18**, 125–134 (2015)

9. Medfar, A., Boujelebene, M., Bayraktar, E.: A mathematical model to choose effective cutting parametrs in electroerosion, EDM. J. Achiev. Mater. Manifact. Eng. **47**(1), (2011)
10. Tebni, W., Boujelebene, M., Bayraktar, E., Ben Salem, S.: Parametric approach model for determing electrical discharge machining (EDM) conditions, effect of cutting parameters on the surface integrity. Arabian J. Sci. Eng. **34/1c**, 101–114 (2009)
11. Ozkul, I., Berat Baris, B., Adnan, A.: Machinability of sleipner cold work stell with wire electric discharge machining. Int. J. Elect. Mech. Mechatronic Eng. **2**(3), 252–260
12. A. A. Khan, S.E. Saifuddin, Wear characteristics of copper and aluminium electrodes during EDM of stainless steel and carbide, Proceeding of the international conference on Mechanical Engineering Dhaka, Bangladesh (2005)
13. Prabhu, S., Vinayagam, B.K.: Analysis of surface characteristics of AISI D2 tool steel material using electric discharge machining process with single wall carbon nano tubes. IACSIT Int J. Eng. Technol. **2**(1), (2010)
14. Guu, Y.H.: AFM surface imaging of AISI D2 steel machined by the EDM process. Apple. Surface Sci. **242**(2004.) (ICME05-AM-09]), 245–250 (2005)
15. AY, M., Aydogdu, D.: Tel erozyomda Kesma paranehinin parçain bayut olçuusume et kilerinin denyesel ineelennesi. Makine teknolojileri Electronik Deigisililt. **7**(13), 31–44 (2010)
16. Farnaz Nourbakhsh, K.P., Rajurkar, A.P.M., Cao, J.: Wire electro-discharge machining of titanium alloy. Procedia CIRP. **5**, 13–18 (2013)
17. Tosun, N., Cogun, C., Tosun, G.: A study on kerf and material removal rate in wire electrical discharge machining based on taguchi method. J. Mater. Process. Technol. **152**, 316–322 (2004)
18. Rajesh, R., Dev Anand, M.: The optimization of electro-discharge machining process using response surface methodology and genetic algorithms. Procedia Eng. **38**, 3941–3950 (2012)
19. Chalisgaonkar, R., Kumar, J.: Multi-response optimization and modeling of trim cut WEDM operation of commercially pure titanium (CPTi) considering multiple user's perferences. Eng. Sci. Technol. Int. J. **18**, 125–134 (2015)
20. GS Paix Méthodes Taguchi, une approche pratique. Addision-Wesley, MA (1992)
21. Boujelbene, M., Bayraktar, E., Tebni, W., Ben Salem, S.: Influence of machining parameters on the surface integrity in electrical discharge machining. Arch. Mater. Sci. Eng. **37**(2), 110–116 (2009)